Marine and Petroleum Geology 166 (2024) 106900

Contents lists available at ScienceDirect

Marine and Petroleum Geology

journal homepage: www.elsevier.com/locate/marpetgeo

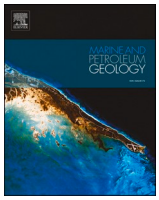

Quaternary sedimentation rate revealed by semi-quantitative analysis in global ocean

Tianyu Huang [a,b], Chao Ma [a,b,d,e,*], Siding Jin [b,c,**], Yida Yang [f], Xiumian Hu [g], Mingcai Hou [a,b]

[a] State Key Laboratory of Oil and Gas Reservoir Geology and Exploitation & Institute of Sedimentary Geology, Chengdu University of Technology, Chengdu University of Technology, Chengdu, 610059, China
[b] Key Laboratory of Deep-Time Geography and Environment Reconstruction and Applications of Ministry of Natural Resources, Chengdu University of Technology, Chengdu, 610059, China
[c] College of Energy, Chengdu University of Technology, Chengdu, 610059, China
[d] College of Computer Science and Cyber Security, Chengdu University of Technology, Chengdu, 610059, China
[e] Geomathematics Key Laboratory of Sichuan Province, Chengdu, 610059, China
[f] School of Earth Sciences and Resources, China University of Geosciences, Beijing, 100083, China
[g] School of Earth Sciences and Engineering, Nanjing University, Nanjing, 210023, China

ARTICLE INFO

Keywords:
Oceanic sediments
Spatiotemporal evolution
Lithology
Polynomial fitting
Paleoclimate

ABSTRACT

The sedimentation rate (SR) of oceanic sediments can be understood as the layer thickness accumulated by marine sediments in a certain period of time. The study of SR in the global ocean is pivotal for understanding key aspects such as oceanic water energy, climate dynamics, terrestrial input, marine environment, and ecosystems robustness. However, the evolution characteristics of oceanic sediment SRs at continuous time and spatial scales are still lacking. This research employs a creative polynomial fitting approach, distinct from conventional average SR computations, to achieve higher resolution SR analysis. This research extensively examines SR variations across temporal, spatial and lithological dimensions. Utilizing a comprehensive dataset from 343 globally distributed (DSDP, ODP, IODP), including detailed lithology data from 99 sites, we reconstruct the evolutionary history of Quaternary oceanic sediment SR. Our findings uncover diverse sedimentation trends across different oceanic environments. A notable inverse correlation emerges between SR and both the proximity to continental margin and the depositional period, substantiated by robust quantitative and semi-quantitative evidence. Additionally, a significant correlation between SR and lithology is observed. We identified the SR of terrigenous clastic sediments is obviously related to their size, alongside a clear latitudinal differentiation in biogenic SR between the northern and southern hemispheres. In the northern hemisphere, SR increase with latitude, marked by a transition from calcium-based to silica-based biogenic sediments. Conversely, in the southern hemisphere, SRs decrease with latitude following a same transition. This pattern reflects the habitat preferences of diverse marine organisms and the greater land area in the Northern Hemisphere. Additionally, we've developed a semi-quantitative method for the relationship between sediments and SR considering factors such as distance to continental margins, ocean and latitude. This method contributes valuable insights to geological research.

1. Introduction

The investigation of sedimentation rates (SRs) in ocean sediments is a cornerstone in Earth science, offering unparalleled insights into ocean dynamics, climate history and environmental change. SRs, especially during the Quaternary (2.58–0 Ma), provide a window into the past, revealing the complex interplay between climates change (Molnar and England, 1990; 2001, 2004; Zhang et al., 2001), lithology (Ibach, 1982; Levitan et al., 2012), tectonics (Schwab, 1976; Sadler, 1981; Donnelly, 1982; Cochran, 1990), glacier changes(Baas et al., 1997; Backman et al., 2004), sea ice variability (Moran et al., 2006; Polyak et al., 2009; Liu et al., 2012), monsoons (Chen et al., 2017), ocean currents (Goldberg

* Corresponding author.
** Corresponding author.
E-mail addresses: machao@cdut.edu.cn (C. Ma), jinsiding@cdut.edu.cn (S. Jin).

https://doi.org/10.1016/j.marpetgeo.2024.106900
Received 15 January 2024; Received in revised form 24 April 2024; Accepted 13 May 2024
Available online 16 May 2024

and Griffin, 1964; Worsley and Davies, 1979a; Davies et al., 1995), precipitation patterns(Gard, 1993), weathering conditions (Goldberg and Griffin, 1964; Bacon, 1984), sea level fluctuations (Worsley and Davies, 1979b; Baas et al., 1997), and paleobiological fossils (Schott, 1939; Liu et al., 2012; Dutkiewicz et al., 2015). Quaternary was a time of dramatic geological and biological evolution, characterized by the formation of continents, deep-sea basins, active volcanoes, and high mountains. It was a period marked by the widespread ice sheets and significant climate changes, which fostered rapid biological evolution (Ericson and Wollin, 1968). In contrast to the terrestrial environment, sediments accumulated on the seafloor in a slow but relatively uninterrupted manner throughout the Quaternary (Bell and Walker, 2014). The consequential environmental transformations, recorded in marine sediments and geological formations, are evident through the preservation of paleobiological fossils. These historical archives render the study of Quaternary Ocean sediments and their SRs of profound scientific importance (Chen et al., 2017). Given their relatively recent geological age, Quaternary sediments often lack lithification, resulting in a loose and unconsolidated state. This aspect reduces the potential for errors caused by compaction and deposition interruptions when calculating SRs, thereby enabling more accurate and realistic assessments (Davies et al., 1977; Anderson et al., 2013). Quantitative analyses of SRs in Quaternary Ocean sediments are invaluable for understanding the ancient oceanic environments and paleoclimatic evolution. They also play a crucial role in fields such as shale oil and gas exploration (Zhou et al., 2009; Zhang et al., 2013), and astrochronological research (Li et al., 2018). Moreover, these studies serve as essential references for comprehensive global investigations of SRs across extended geological periods.

Despite significant advancements in global SR data collection, as exemplified by Restreppo et al. (2020), and the macroscopic understanding of seafloor sediment distribution by Dutkiewicz et al. (2016), the quantitative relationship between SRs and lithology in oceanic environments remains unclear. This gap is compounded by the significant challenges in gathering raw data necessary for calculating SRs. The complexity and extensive labor required to collect these indicators have led to a notable scarcity in quantitative research that explores SRs on a continuous timescale with high resolution, particularly on a global scale. Further complicating this research landscape is the dispersed nature of global ocean sediment lithology data. Such data are often fragmented across a wide array of publications and databases, presenting a heterogeneous that poses considerable hurdles in data collection and consolidation efforts (Ma et al., 2021). Here, the study utilizes age-depth data from 343 sites of ocean drilling programs (DSDP, ODP, IODP) and lithology data from 99 sites from IODP stages. These sites contain comprehensive information dating back to the Quaternary, providing a solution to the challenges proposed above, such as the temporal and spatial evolution characteristics of SRs in oceanic sediments in continuous time and spatial scale, as well as the coupling relationship with lithology.

This paper aims to use the age depth data set and lithology data from ocean drilling voyage reports to address the following objectives: (i) calculate the average SRs for the five major global oceans since the Quaternary (2.58–0 Ma) and examine the factors influencing these rates; (ii) quantify the relationship between distance to continental margins and SRs at different time points (0.5 Ma, 1 Ma, 1.5 Ma, 2 Ma, 2.5 Ma) and the relationship between water depth and SRs, analyzing the factors responsible for these variations; (iii) compute the SR ranges for three primary sediment categories—terrigenous clastic, biogenic, and carbonate sedimentary rocks—and evaluate the spatiotemporal response of SRs for these lithologies.

2. Materials and methods

2.1. Data presentation

Sediment cores from DSDP/ODP/IODP serve as our prime archive for obtaining continuous records with well-established chronologies. Sediment from pelagic or semi-pelagic sites also help mitigate potential biases from turbidite sequences. We review all Initial Reports volumes up through IODP Expedition 382 to select sites suitable for this study. Chosen sites needed to have ample data of sufficient quantity, ideally with complete or near-complete sediment sections cored for the Quaternary, with preference given to sites covering older periods.

Initially, we screened 1000 sites with good age model data from the Deep Sea Drilling Project (DSDP, Leg1-96), Ocean Drilling Project (ODP, Leg100-210), and International Ocean Discovery Program (IODP, Expedition nos. 301–312, 317–382). At each site, we selected the most suitable hole from each ocean expedition. From these, 343 sites (343 holes) were identified (Fig. 1, light blue dots) with available age and depth data covering the Quaternary. We adhere to the standards of the Geological Time Scale 2020; GTS 2020) for age data. These sites span all major ocean basins and various depositional environments, including regions with significant terrestrial sediment input, areas of intense upwelling with high primary productivity, and pelagic and semi-pelagic, carbonate-rich, open ocean areas, among others. Similarly, lithology data from 99 holes across 99 IODP sites were also obtained and analyzed, and these holes contain more complete Quaternary lithological data (Fig. 1, pink dots). Furthermore, we have collected data on the water depth (approximate modern water) for these 99 holes to be used in subsequent analysis and discussions. The detailed attributes of the data are provided in the attachment (Supplementary data). Analysis of cruise report proceedings revealed that most hole's lithological characteristics are expected to show large, continuous distributions. Therefore, for the complied lithological data obtained, after arranging them in ascending depth order, we excluded any lithological data appearing only at specific depth point instead of within depth intervals.

2.2. Sedimentation rate calculation

Traditional methods for calculating SRs mostly rely on average SRs, such as determining absolute ages of rocks through methods like radiocarbon dating, zircon U–Pb dating, K–Ar dating, Rb–Sr dating, and high-precision Re–Os isotope dating (Anderson et al., 2013; Zhang et al., 2023). By using the ratio of differences in depth and age, the average SR over a certain period can be calculated. However, these dating methods are costly and not universally applicable, yielding only average SRs. Additionally, utilizing cyclostratigraphy and astronomical dating methods can depict high-resolution SRs, but uncertainties in parameter adjustments and the selection of theoretical astronomical cycle models limit their universality (Zhang et al., 2023). Consequently, based on the characteristics of Quaternary sediments and the collected DSDP, ODP, and IODP data, we believe that a polynomial approach and alignment for the first derivative to calculate SRs is more appropriate due to its adaptability and accuracy (Li et al., 2023). as illustrated in Fig. 2. In addition, the advantages of using polynomial fitting to calculate the SR and the specific details of the formula can be found in the supplementary. To prevent overfitting, we set the polynomial fitting order to range from 1 to 6, and the fitting order is taken to ensure that the fitting curve is monotonous and the R-square value is large. The SRs are measured in cm/kyr. This approach enables us to determine SRs for 343 holes with appropriate time resolution, as well as ages and SRs for 99 holes across various lithologies.

It is essential to verify the calculated results of SRs. Original cruise reports typically provide average SRs between two depths, which may be restrictive for high-resolution time scale studies. In contrast, our polynomial fitting yields a continuous curve, allowing for derivation of SRs that should exhibit gradual transitional characteristics. As long as

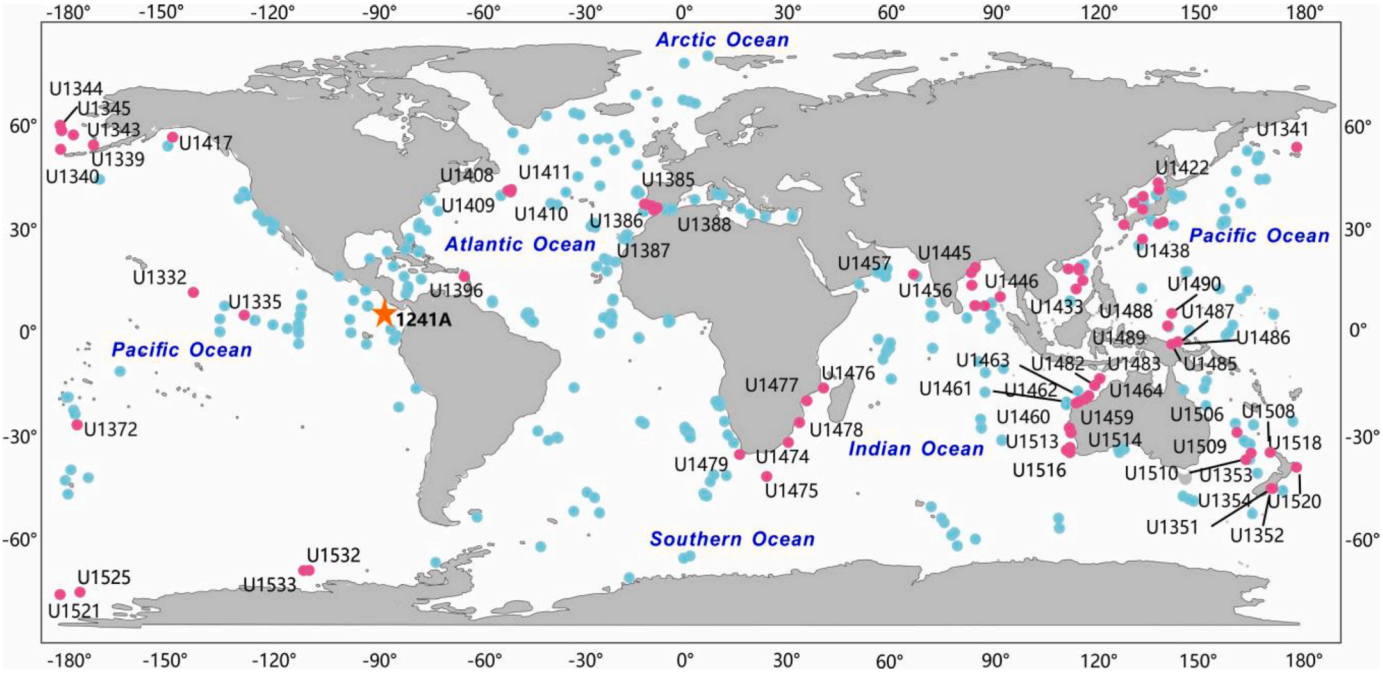

Fig. 1. Geographic distribution of research sites. This map illustrates a total of 343 study sites, marked in light blue, and an additional 99 sites, marked in pink, specifically analyzed for lithological composition in this research.

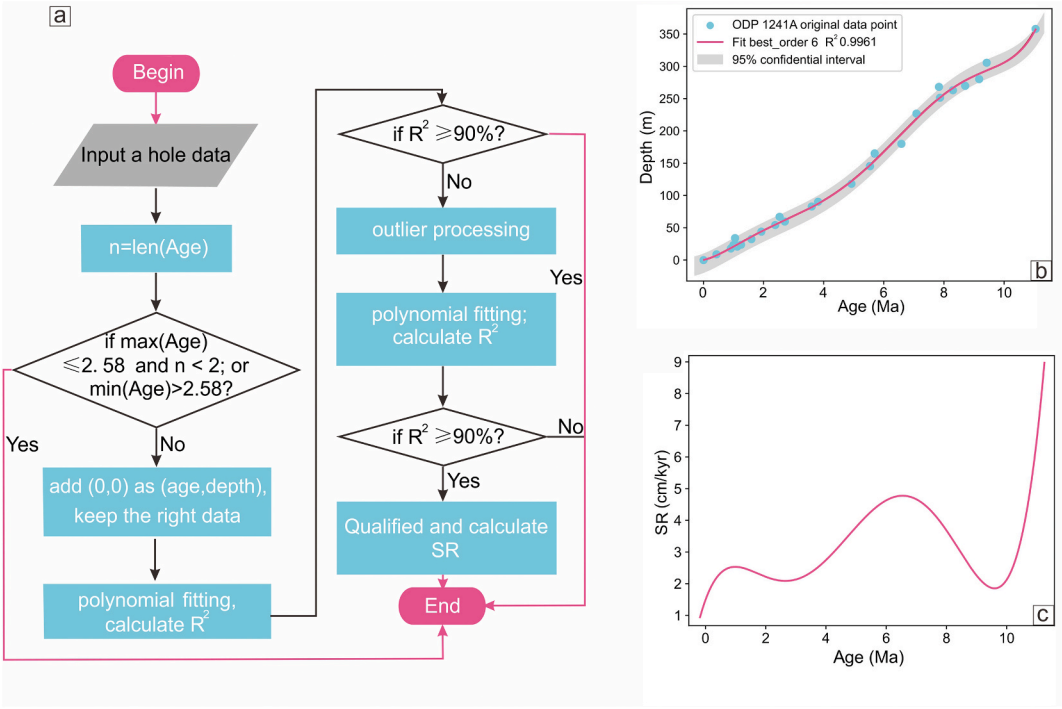

Fig. 2. Overview of the SR calculation methodology. (a) Depicts the algorithm flowchart used for calculating SR. (b) Presents a polynomial fitting process, exemplified using data from Hole 1241A, the location of Hole 1241A is indicated by an orange star in Fig. 1. (c) Shows the resulting first derivative of the polynomial in (b), representing the magnitude of the SR.

the polynomial fitting is effective and overfitting is minimized, we can ascertain instantaneous SRs at a reasonably higher time resolution. It is acknowledged that SRs calculated via polynomials might contain some level of error. To validate our calculated rates, we will compare SRs reported in the original cruise reports. If the rates in these reports fall outside our calculated range, we will consider refitting the data or using the average rate from the cruise reports as the instantaneous rate for that particular hole within a specific depth range.

2.3. Lithology classification

To streamline the statistical analysis of lithology in this study, we initially undertook data preprocessing for all lithological data. This involved standardizing data to the predominant lithology and

simplifying them to their most concise form based on lithological features. For instance, "calcareous bearing clayey silt" or "calcareous bearing clayey silt with nannofossils" are both simplified to "clayey silt", given the predominance of this component. Changes in the nomenclature of other sediment types and the finalized list of adopted sediment types are detailed in Appendix Table1. Subsequently, the lithological data are classified into three major categories based on their source and lithological properties: terrigenous clastic sediments, biogenic sediments, and carbonate sedimentary rocks (Dutkiewicz et al., 2015).

Terrigenous clastic sediments encompass 15 types: sand, silty sand, muddy sand, clayey sand, fine sand, interbedded sand and mud, sandy silt, silt, clayey silt, sandy mud, silty mud, mud, sandy clay, silty clay, and clay. Their data volume accounts for Fig. 3a. These originate from land and are deposited on the seabed following process of weathering, erosion, and transportation. Sand, a granular material, consists of finely divided rock and mineral particles, primarily quartz in non-tropical and continental settings. Silt, with a particle size between sand and clay, primarily comprises quartz and feldspar. It can exist as soil or suspended sediment in water bodies. Mud is a water-soil mixture, including silt and clay, which can harden into sedimentary rocks like shale or mudstone over time. Clay consists of tiny, electrostatically bonded, plate-shaped particles.

Biogenic ooze, a pelagic sediment containing over 30% skeletal material, exists mainly as either carbonate or siliceous ooze. Carbonate ooze covers about half of the world's seafloor, found chiefly above depths of 4500 m where it does not dissolve quickly. Siliceous ooze, less common, is primarily found around Antarctica and near the Equator. This paper studies four types of biogenic sediments: biosiliceous ooze, calcareous ooze, foraminiferal ooze, and nannofossil ooze.

Carbonate rocks, predominantly made of minerals like calcite and dolomite, vary in texture according to Dunham's 1962 classification, from crystalline to mudstone. This paper analyzes SRs of grainstone, packstone, wackestone, and mudstone. Grainstones are formed by dynamic aquatic processes, whereas packstones develop in zones with varying energy levels. Wackestones consist of particles transported into calmer settings, and mudstones form in still environments, influenced by chemical, biological, or mechanical factors. Marl, rich in carbonate minerals, clays, and silt, forms in aquatic environments, often involving algae, and solidifies into marlstone.

For each category, polynomial fitting is applied to the depth data corresponding to their specific lithologies, utilizing age-depth data from the same hole. This step is crucial for determining the age and SR at the corresponding depths for each lithology within the same hole, thereby enabling more detailed analysis and investigation. The distribution and proportions of these three sediment types, along with the top several sediment types within each major category, are depicted in Fig. 3., providing a clear visual representation of our findings.

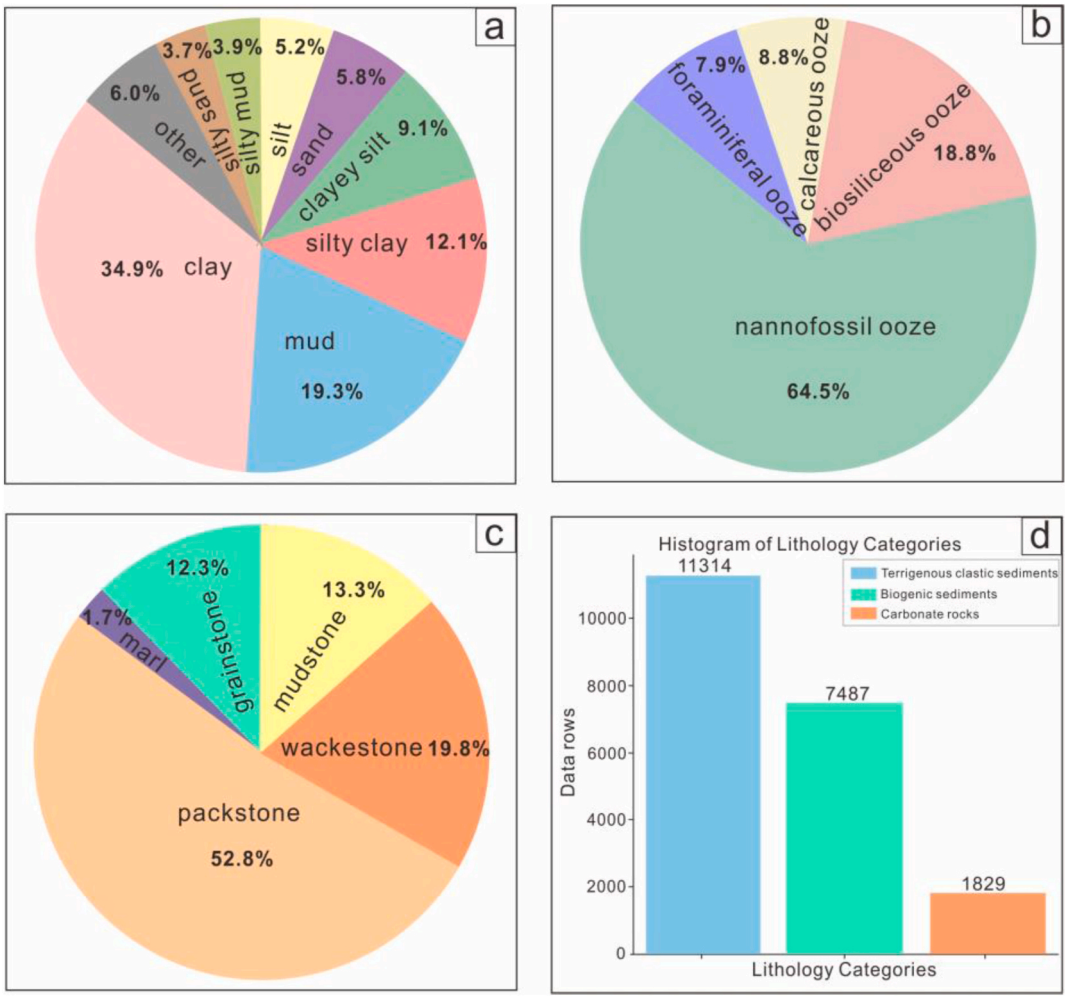

Fig. 3. Distribution and proportions of lithologic categories. (a) Illustrates the proportion of terrigenous clastic sediments. (b) Shows the lithologic proportions in biogenic sediments. (c) Details the lithologic composition within carbonate rocks. (d) Displays the overall data quantity for the three primary lithologies.

3. Results

3.1. Average sedimentation rates of five oceanic basins

Informed by a comprehensive literature review, it's understood that SRs variations are often intricately linked to climate and tectonic activities (Whitman and Davies, 1979; Zhang et al., 2001; Molnar and England, 1990). Accordingly, this study selected 8 time points in Quaternary, marked by significant geological events and climate shifts, to calculate the average SRs across five major oceans at specific intervals (0.15Ma, 0.6Ma, 0.9Ma, 1.2Ma, 1.3Ma, 1.7Ma, 2.2Ma, 2.5Ma) (Donnelly, 1982; Zhu et al., 2012; Diesing, 2020).

The calculated average SRs at these 8 time points (Fig. 4) reveal a consistent trend in the Atlantic, Pacific, and Indian Oceans since the Quaternary. However, the Arctic and Southern Oceans exhibit distinct differences due to their unique geographical locations and climatic conditions. In the Arctic Ocean, the average SR increased from 3.75 cm/kyr to 5.57 cm/kyr between 2.5 and 1.3 Ma, followed by a decreased to 4.66 cm/kyr. This rate is slightly higher in the late Quaternary compared to the early period. In the Southern Ocean, a gradual decline from 1.66 cm/kyr to 1.51 cm/kyr was observed from 2.5 to 2.2 Ma. Between 2.2 and 1.2 Ma, the rate increased to 2.16 cm/kyr, the highest in the Quaternary. It then decreased to 1.44 cm/kyr from 1.2 to 0.6 Ma, before rising to 1.82 cm/kyr, slightly higher than the early Quaternary. In contrast, the Atlantic, Indian and Pacific Oceans showed a gradual increase in SR from 2.5 to 1.3 Ma. Notably, after 1.2 Ma, the Indian Ocean displayed a rapid acceleration in SRs, significantly surpassing those of the Atlantic and Pacific Oceans.

3.2. Relationship between distance to continental margin and sedimentation rate

In this study, we used the nearest neighbor analysis method in ArcGIS statistical tools to calculate the shortest distances from 343 holes to the nearest continental margin (Fig. 5a; b; c). The kernel density estimate plot (Fig. 5d) of distances from these 343 holes to the nearest continental margin shows a trend that with the distances to the continental margin, the number of holes is gradually reduced and meets the heavy tail distributions. Even though SR generally decreases with distance to the continental margin, it is possible that sediments at close distances may have been transported over long distances (Clift et al., 2008; Peketi et al., 2021).

We conducted calculations for the SRs at various geological ages (0.5 Ma, 1 Ma, 1.5 Ma, 2 Ma and 2.5 Ma) for the 343 holes and five geological time points were fitted with logarithmic curves to represent the relationship between SRs and distances to continental margins (Fig. 5e). An exploration of relationship between SRs and distances to the nearest continental margin was subsequently carried out for each time point.The influence of age on SR varies across different distance ranges (Appendix Table 2). At the five time points, the relationship between SR and distance can be divided into four stages: (1) Stage One: For distances greater than 1.85×10^3 km, the SRs in increasing order are at 1.5 Ma, 1 Ma, 2 Ma, 0.5 Ma, and 2.5 Ma. (2) Stage Two: Within the distance range of $1.2–1.85 \times 10^3$ km, the SRs in increasing order of time are 1.5 Ma, 1 Ma, 2 Ma, 2.5 Ma, and 0.5 Ma. (3) Stage Three: For distances between 0.67 and 1.2×10^3 km, the rates in increasing order of time are 1.5 Ma, 2 Ma, 2.5 Ma, 1 Ma, and 0.5 Ma. (4) Stage Four: When the distance is less than 0.67×10^3 km, the rates in increasing order of time are 2.5 Ma, 2 Ma, 1.5 Ma, 1 Ma, and 0.5 Ma.

3.3. Relationship between lithology and sedimentation rate

3.3.1. Terrigenous clastic sediments

(i) Globally: Relationship between lithology and SR

The terrigenous clastic sediments are labeled 1–15 according to their size from largest to smallest and are respectively sand, silty sand, muddy sand, clayey sand, fine sand, interbedded sand and mud, sandy silt, silt, clayey silt, sandy mud, silty mud, mud, sandy clay, silty clay, clay. We have produced box plot for 15 types of terrigenous clastic sediment SRs (Fig. 6a) and SR kernal density estimates for four typical terrigenous clastic sediments: sand, silt, mud, clay (Fig. 6b). It can be observed that the SR of sediments ending in clay increases with size; those ending in mud generally increase as size increases; similarly, sediments ending in silt show a rough increase with size; only the median SR of sand significantly decreases as size increases. The bulk density estimation charts for these four sediment types also exhibit a characteristic pattern. The peak of a kernal density curve indicates where the data is most densely concentrated. Apart from sand, which has a smaller first peak, the first peak values in the SR bulk density chart for the other three sediment types increase with particle size: 5.09 cm/kyr, 25.84 cm/kyr, and 35.72 cm/kyr (Fig. 6b). Both clay and sand, exhibit multiple peaks in their bulk density estimation charts, indicating areas of concentrated SR data. Sand shows peaks at 9.11 cm/kyr, 42.95 cm/kyr, 61.3 cm/kyr, while clay has peaks at 5.09 cm/kyr, 65.26 cm/kyr, and 83 cm/kyr (Fig. 6b). These peaks represent a clearer view of the overall distribution of SR for each sediment type.

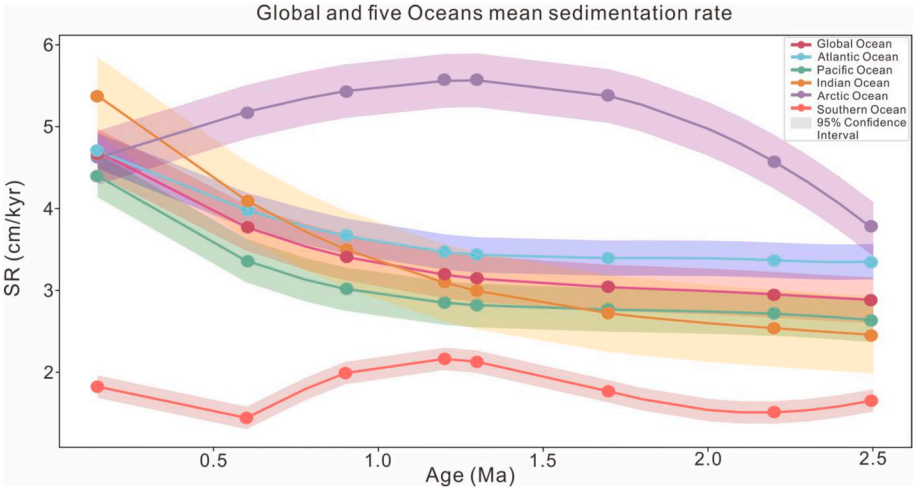

Fig. 4. Map of mean sedimentation rates of oceanic sediments across the five major oceans worldwide.

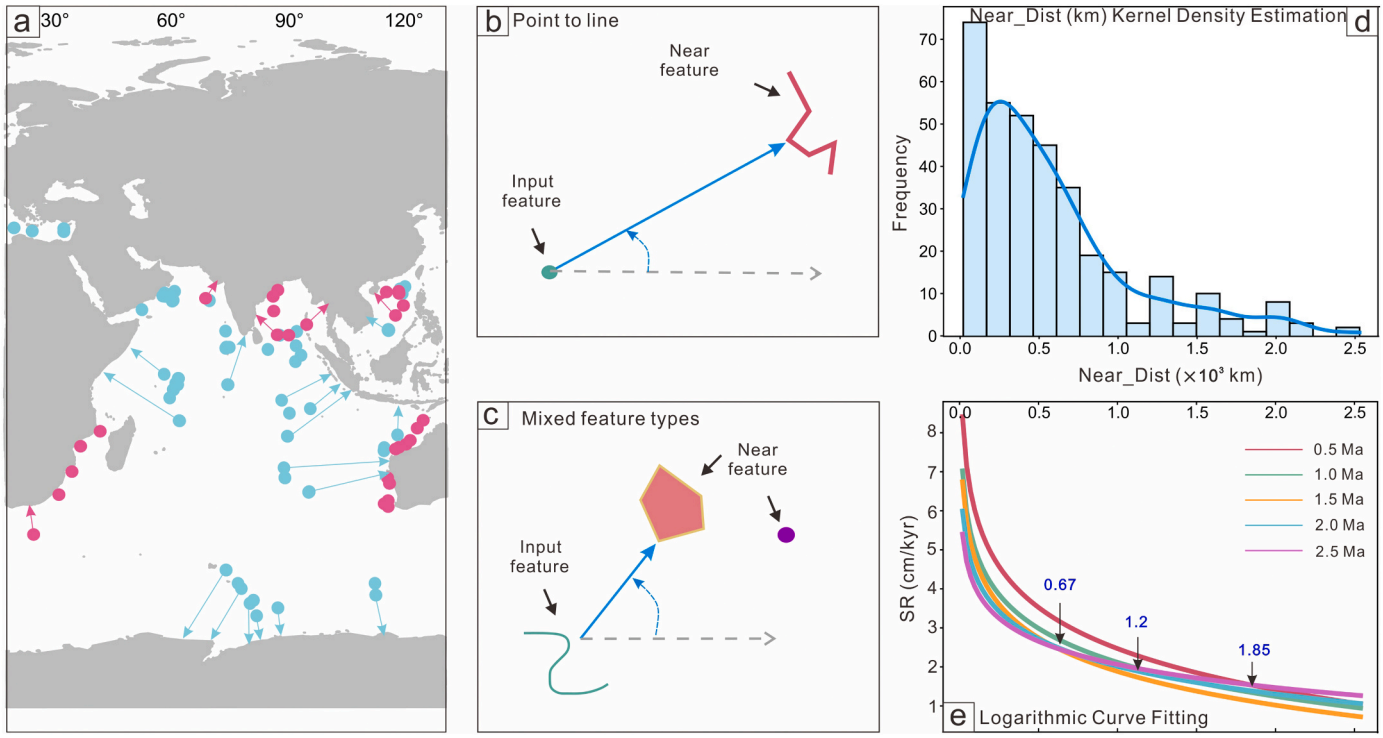

Fig. 5. Analysis of the relationship between SR and distance to continental margins. (a) The light blue and pink dots represent the position of the holes, and the arrows represent the distance from the holes to the continental edge. (b; c) Schematic representation of the nearest neighbor algorithm used in ArcGIS. (d) Kernel density estimation plot demonstrating the distribution of distances (in kilometers) from all drill holes to the nearest continental margin. (e) Graph illustrating the correlation between SR and distance over fixed time points (0.5 Ma, 1 Ma, 1.5 Ma, 2 Ma, 2.5 Ma).

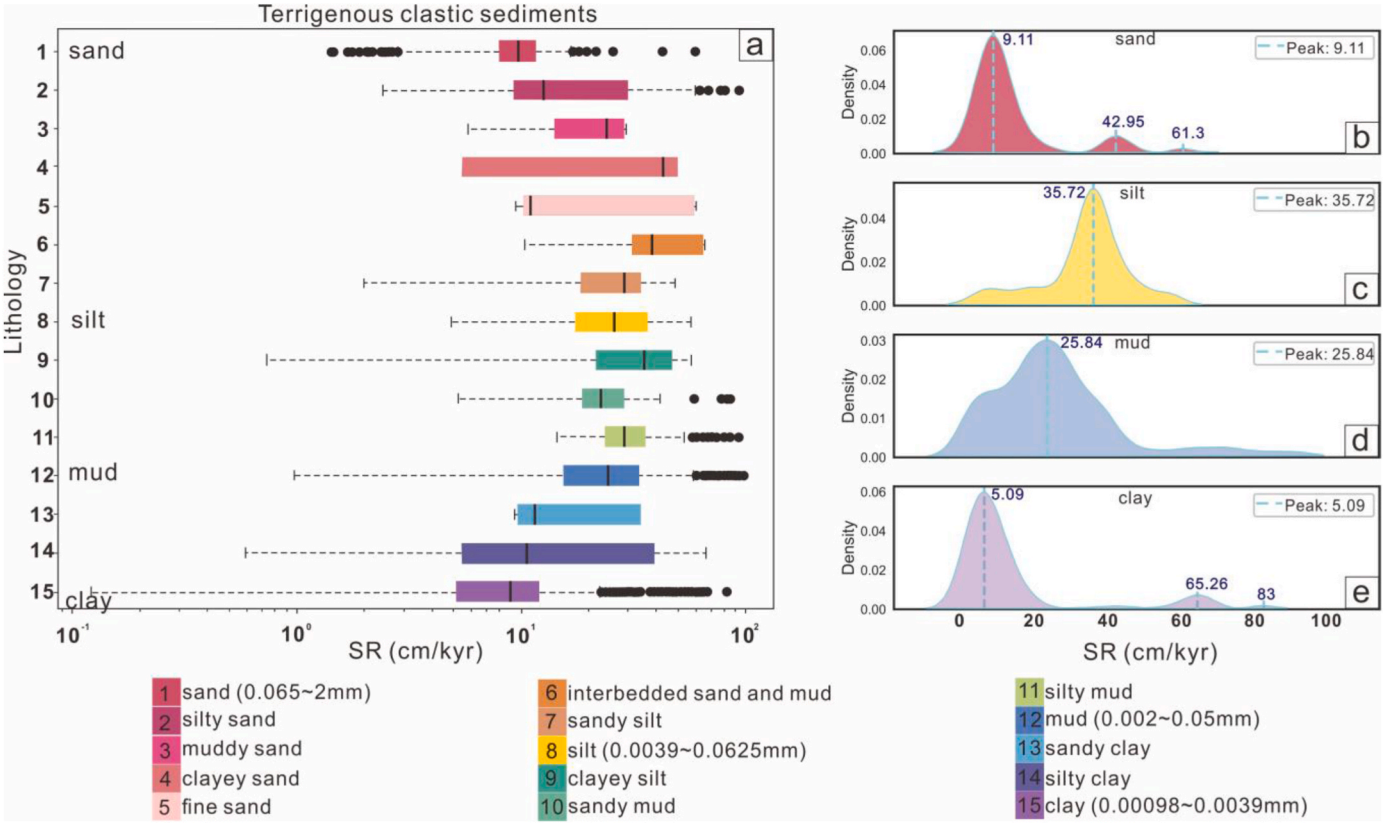

Fig. 6. Quaternary SR ranges for terrigenous clastic sediments in global oceans. (a) This chart displays the SR ranges for 15 types of terrigenous clastic sediments during the Quaternary. The horizontal axis is logarithmic. (b) Kernal density estimation map of SR in sand. (c) Kernal density estimation map of SR in silt. (d) Kernal density estimation map of SR in mud. (e) Kernal density estimation map of SR in clay.

(ii) Regional scale: Relationship between lithology, distance, water depth and SR

Based on the distance of 15 types of terrigenous clastic sediments from the continental margin, they are categorized into nine groups to investigate the relationship between the SR of different terrigenous clastic sediments and their proximity to the continental edge, as well as their relationship with the water depth (approximate mean modern water depth) at the time of sedimentation (Fig. 7). The SR of terrigenous clastic sediments exhibits a general negative correlation with increasing water depth across different distances from the continental margin. Specific details are outlined below.

Group1: Within 20–70 km from the continental margin, diverse sediment types are observed. Median SR initially increases then decreases with decreasing particle size. Water depth decreases then increases, generally below 1500 m.

Group 2: Within 70–120 km from the margin, sediment types resemble Group 1. Median SR decreases for various sediments compared to Group 1, except for fine sand and interbedded sand and mud. SR follows a pattern of initial increase, decrease, then increase with water depth fluctuations.

Group 3: Within 120–170 km, fewer sediment types are observed, including silt and sandy clay. Median SR decreases for silty clay and clay compared to Group 2, while SR increases for clayey silt. Water depth shows an initial decrease followed by an increase.

Group 4: Within 170–220 km, fewer sediment types compared to Group 3. Median SR increases for silt and clay but decreases for clayey silt and silty clay. Water depth follows a similar trend.

Group 5: Within 220–250 km, an increase in sediment types is observed. Median SR decreases for silt and clay but increases for clayey silt and silty clay. Water depth generally increases, particularly when median SR for silt is low.

Group 6: Within 300–400 km, an increase in sediment types is observed. Median SR decreases for silty sand and clay but increases for sandy silt, silt, clayey silt, and silty clay. Water depth fluctuates, generally above 2500m.

Group 7: Within 400–500 km, an increase in sediment types with reduced quantities is observed. Median SR decreases for various sediments, and the SR range narrows. Water depth is generally close to 4000m.

Group 8: Within 500–700 km, a reduction in sediment types is observed, with median SR generally less than 10 cm/kyr. Water depth remains stable, close to 4000m.

Group 9: Beyond 700 km, a sharp reduction in sediment types, with only clay present. Median SR is less than 1 cm/kyr, and water depth approaches 5000m. The specific SR range and other statistic parameters such as min, Q1 (the first quartile), median, Q3 (the third quartile), max and mean in different distance ranges for each lithology are available in Appendix Table 3 and Appendix Table 4.

(iii) Regional scale: Relationship between lithology, water depth, slopes and SR

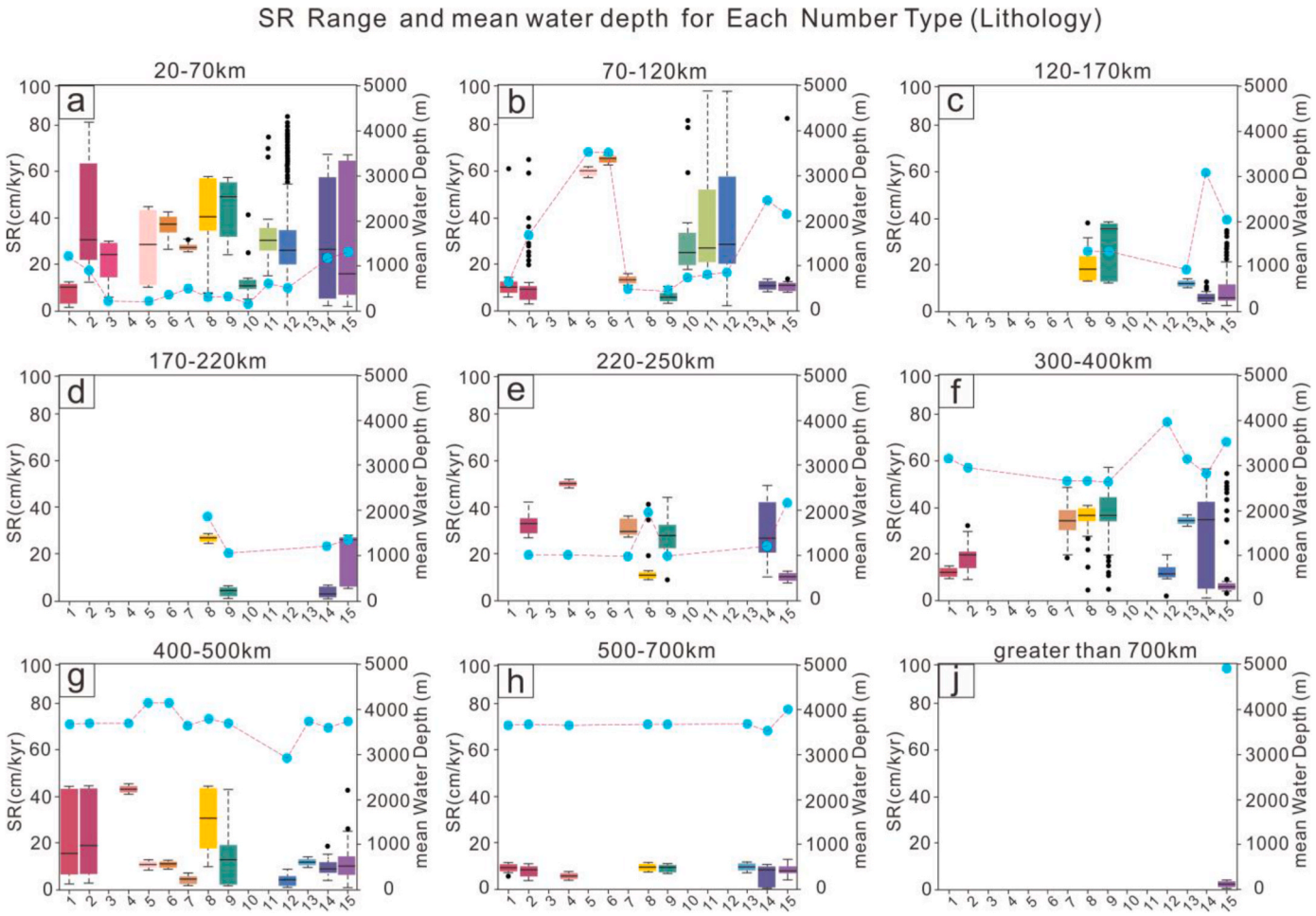

Fig. 7. SR variations of terrigenous clastic sediments relative to distances from continental margins and water depth. Refer to Fig. 6 for lithology legends 1–15. This figure delineates the box plot of SRs for various types of terrigenous clastic sediments at different proximities to the nearest continental margins. The light blue dots represent the mean water depth for this lithological data. Panels (a) to (j) illustrate the SRs across nine different distance ranges for these terrestrial clastic sediments.

In different water depth ranges (Fig. S1), there are distinct trends in the relationship between water depth, terrigenous clastic sediments, and SR. Generally, as water depth increases, the SR of terrigenous clastic sediments tends to decrease. The relationship between water depth and distance to the continental margin (Fig. S2) predominantly shows a positive correlation across four distance ranges. Considering the influence of slopes on terrigenous clastic sediments, we calculated the tangent of the slope angle (tanθ) as the ratio of water depth to distance to the continental margin (supplementary data3). The maximum value, 0.0075, is less than 0.0175 (tan1°), approximating a plain (Tan et al., 2022). Thus, this study temporarily disregards the influence of slopes on the SR of terrigenous clastic sediments.

3.3.2. Biogenic sediments

In the Northern Hemisphere, the primary sediment types and SR vary by latitudes. **At low latitudes (0–30°N)**, sediment types include calcareous ooze (1.46–16.04 cm/kyr), nannofossil ooze (0.24–17.56 cm/kyr). **At mid-latitudes (30–60°N)**, sediment types such as nannofossil ooze (0.46–56.17 cm/kyr), foraminiferal ooze (0.46–1.68 cm/kyr), calcareous ooze (3.65–57.31 cm/kyr), biosiliceous ooze (3.44–55.48 cm/kyr). **At high latitudes (60–90°N)**, the main sediment type is biosiliceous ooze (49.27–49.74 cm/kyr). In the Southern Hemisphere, the main lithology types and significant variations in SRs differ considerably across different latitudes. **At low latitudes (-30~0°S)**, sediment types include foraminiferal ooze (0.26–16.87 cm/kyr), nannofossil ooze (1.26–9.80 cm/kyr). **At mid latitudes (-60~-30°S)**, sediments types such as calcareous ooze (0.59–2.83 cm/kyr), foraminiferal ooze (1.08–9.28 cm/kyr), nannofossil ooze (0.37–8.99 cm/kyr). **At high latitudes (-90~-60°S)**, the main sediment type is biosiliceous ooze (0.70–11.37 cm/kyr). The specific details are available in supplementary data5.

We categorize calcareous ooze, foraminiferal ooze and nannofossil ooze as calcareous ooze in Fig. 3b. Globally, the box plot of SR of calcareous and siliceous biogenic sediments were drawn according to latitude (Fig. 8). In the Northern Hemisphere, from low to high latitudes, the type of biogenic sediment transitions from calcareous to siliceous, and the median of SR gradually increase. In the Southern Hemisphere, from low to high latitudes, the type of biogenic sediment also transitions from calcareous to siliceous. However, the median SR of calcareous biogenic sediments decreases with latitude increases. The median SR of siliceous sediments at high latitudes in the Southern Hemisphere is noticeably lower than that at mid to high latitudes in the Northern Hemisphere. Additionally, the range of SR for biogenic sediments (as indicated by the length of the box in box plots) in mid to high latitudes of the Northern Hemisphere exceeds that in the Southern Hemisphere. This approach allows for a comprehensive understanding of the SRs and characteristics of biogenic sediments, accounting for the variability due to latitude and environmental factors.

3.3.3. Carbonate sedimentary rocks

During the Quaternary on a global scale, the study identified the following carbonate sedimentary rock types along with their respective SR ranges: marl (4.20–27.55 cm/kyr), mudstone (2.32–27.10 cm/kyr), wackestone (0.26–29.76 cm/kyr), packstone (0.89–29.02 cm/kyr), and grainstone (0.79–27.76 cm/kyr). After arranging these carbonate rocks – grainstone, packstone, wackestone, mudstone, and marl in order from largest to smallest grain size, there is an increasing trend in their SR medians (Fig. S3). Detailed statistics for each lithology type, including minimum, Q1, median, Q3, maximum, and mean SR, are provided in Appendix Table 6.

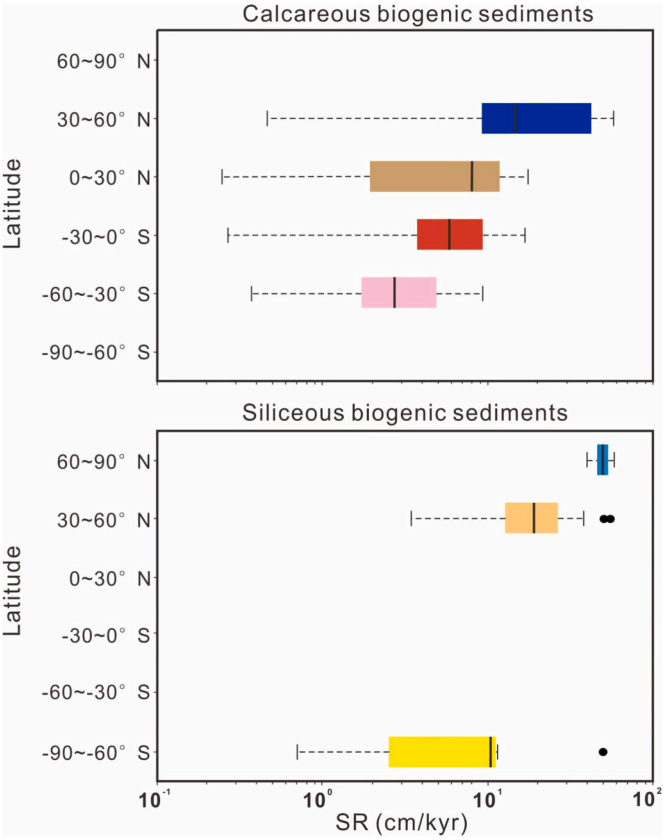

Fig. 8. Box plot of SRs of calcareous and siliceous biogenic sediments. (a).Box plot of SR of calcareous biogenic sediments. (b). Box plot of SR of siliceous biogenic sediments.

4. Discussion

4.1. Key factors influencing Quaternary global oceanic SRs

4.1.1. Climate-induced variations in SRs

Since the Quaternary, overall, comparing the mean SRs of the five oceans at late Quaternary to those at present, there has been a discernible upward trend in the average SRs of the world's five major oceans, with the Atlantic, Pacific, and Indian Oceans exhibiting particularly obvious increases. This trend is evidenced by remarkable global consistency in average SR curves (Fig. 4), corroborating findings by (Davies et al., 1977). Across various global environments, including both active and inactive mountain belts, there has been an increase in SRs and sediment grain sizes over the last 2 to 4 Ma. This trend implies an escalation in erosion rates, attributable to climate change as the primary globally synchronous process driving the widespread intensification erosion and deposition (Whitman and Davies, 1979; Zhang et al., 2001; Lü et al., 2016). The formation of the Arctic ice cap in the last 2–4 Ma has precipitated significant global climate changes, leading to fluctuations in temperature, precipitation, sea levels, vegetation, and other factors. These changes likely expedited weathering and sedimentation processes (Wang, 2018). Research by Hay et al. (1988) indicates a substantial increase in terrestrial sedimentation over the past 5 Ma. The rise in SRs is associated with sea level drops during continental ice ages, which allowed rivers to incise continental margins and augment the influx of terrestrial clastic debris. Concurrently, periods of low sea levels coincide with increased SRs of biological sediments, suggesting a pattern of diminished continental chemical weathering during times of higher sea levels (Worsley and Davies, 1979b). Furthermore, the growth of high-altitude glaciers has contributed to heightened incision and erosion in mountainous regions, while shifts in precipitation patterns have likely

influenced erosion rates (Molnar and England, 1990; Zhang et al., 2001). Therefore, the overall trend in the average global ocean SRs since the Quaternary has been characterized by a significant increase.

4.1.2. Non-climatic contributors induced variations in SRs

The acceleration of tectonic movements is a well-established phenomenon in geoscience, known for its significant impact on enhancing erosion and deposition processes (Pang et al., 2009; Wang, 2018). Mountain uplift, in particular, plays a pivotal role in influencing glacier formation (Raymo and Ruddiman, 1992). A notable example of this is the substantial uplift observed in regions such as Tibet and North America, which is believed to have contributed to the formation and intensification of glaciers in the Northern Hemisphere around 2.4 Ma (Bacon, 1984). In addition, the process of mountain uplift inevitably results in increased erosion. This is exemplified by the Late Pleistocene, where significantly higher SRs were observed in the distal part of the Bengal Fan. This suggests that during glacial maxima, the continental shelf was likely completed exposed, resulting in the direct transport of river sediment loads to the continental slope (Cochran, 1990), thus providing a source of sediment for the ocean to deposit. Furthermore, calculations of SRs at different time scales indicate a systematic trend of decreasing average SRs with increasing time scales. The gradient of this trend varies with different tectonic backgrounds (Sadler, 1981).

4.1.3. Comparative study of SRs in diverse oceanic basins

Since the Quaternary, between 2.5 and 1.3 Ma, SRs in the Arctic Ocean have increased from 3.754 cm/kyr to 5.567 cm/kyr, then gradually decreased to 4.662 cm/kyr. This differs slightly from the SR range calculated by Backman et al. (2004) for the Pliocene to Pleistocene in the Arctic Ocean, which ranged from 0.04 to 0.40 cm/kyr, likely due to variations in sampling methodologies and locations of the data we collect, alongside impacts from distinct seasonal sedimentation and sea ice dynamics (Polyak and Jakobsson, 2011; Levitan et al., 2012; Jakobsson et al., 2014). The Southern Ocean, in contrast, shows relatively low SRs, influenced by limited terrestrial sediment input and predominantly glacial processes in Neogene terrestrial sedimentation (Latimer and Filippelli, 2001; Salvi et al., 2006). Meanwhile, the Indian Ocean's average SRs have increased noticeably since 1.7 Ma, surpassing the Pacific and Atlantic Oceans, attributed to its geographical position and geological activities (Fig. 4). Beginning at 2.4Ma, the uplift rate of the plateau began to slow down. At 1.95–1.77Ma, the Tibet Plateau rose again, which is the "Tibetan Plateau movement C stage", this period marks the major adjustment in the plateau's internal and surrounding water systems, and the 0.73Ma Plateau began to rise strongly again. Extensive glaciation on the plateau began between 0.8 and 0.7 Ma. At about 0.65 Ma, the main plateau entered the cryosphere at an attitude of 3000~3500m, and the "maximum glacial period" appeared. The strong uplift of the plateau not only brings a large amount of terrigenous input to the Indian Ocean, but also has a certain impact on climate. Indian monsoon and ocean circulation, all of which have a certain impact on the SR (Zhu et al., 2012). The Atlantic Ocean has also seen a steady increase in SRs since the Quaternary, with deep-sea clay primarily sourced from continental erosion and impacted by transport through rivers and winds (Biscaye, 1965; Kolla et al., 1979; Donnelly, 1982). In the Pacific Ocean, integral to Cenozoic climate evolution, Late Cenozoic sediment accumulation rates in the upper sediments of the Atlantic, Indian, and Pacific Oceans have outpaced earlier periods, with significant increases in terrestrial sedimentation since 5 Ma, notably in the Mississippi Delta since 2 Ma (Hay et al., 1988; Molnar and England, 1990; Singh et al., 2023).

4.2. The coupling relationship between SR and continental margin distance

In sedimentary basins, both modern and ancient, SRs are influenced by plate tectonic environments. Generally, basins located in the central parts of plates tend to have slower SR compared to those near or at the plate margins. For example, mid-plate basins located entirely on top of a single basement type (i.e., cratonic basins) typically have slow SRs (usually less than 0.006 m/kyr), whereas negative areas near the edges of continental blocks and adjacent orojenic moutains have faster SRs. SRs in basins along or adjacent to plate margins almost always exceed 0.04 m/kyr, often much higher than in mid-plate basins (Schwab, 1976). In this study, the distances of all analyzed holes to the nearest continental margin exhibit a significant "heavy-tailed distribution" characteristic (Fig. 5d). This distribution pattern results from the strategic placement of holes in ocean drilling, primarily focused on studying specific regional features such as monsoons, paleoenvironments, and paleoclimates, hence the prevalence of holes near continental margins. A "logarithmic decrease" in SRs is observed as the distance to the continental margin increases.

When the distance from the continental margin is less than 670 km, the chronological order of decreasing SRs is 0.5 Ma, 1 Ma, 1.5 Ma, 2 Ma, and 2.5 Ma (Fig. 5e; Appendix Table 2). This indicates that as we approach the present, SRs increase, suggesting that near the continental margin, the influence of terrigenous input is greatest. Since the Quaternary, with the onset of glacial climates, intensified weathering has increased erosion on land, leading to more terrigenous input (Hay et al., 1988; Molnar, 2004; Lü et al., 2016). In the deeper oceanic regions, where the distance from continental margin exceeds 1850 km, the chronological order of decreasing SRs is 2.5 Ma, 0.5 Ma, 2 Ma, 1 Ma, and 1.5 Ma. This partially reflects the complex mechanism of deep-sea sediment transport and suggests that the intensity of deep-sea currents during different periods may also influence SRs (Whitman and Davies, 1979; Tan et al., 2022). Additionally, in the intermediate region, approximately 670~1850 km from the continental margin, the order of SRs is quite similar, except for some differences at 1 Ma. We believe that these areas are influenced by similar factors affecting SRs.

4.3. SRs response to lithology

4.3.1. SRs response to terrigenous clastic sediments

Overall, the deposition of these terrigenous clastic sediments is significantly influenced by hydrodynamic conditions, proximity to the continental margin, and water depth (Zhu et al., 2012; Cuthbertson et al., 2016; Zhao et al., 2017). At a global spatial scale, sand exhibits deposition median SR characteristics that are inconsistent with those of the other three sediment types: silt, mud, and clay, and the peak of its density estimation curve is smaller (Fig. 6). The impact on different terrigenous clastic sediments also varies across different distance ranges. For larger particles such as sand, silty sand, muddy sand, and clayey sand, the SR decreases with increasing distance from the continental margin. For medium particles such as fine sand, interbedded sand and mud, sandy silt, silt, clayey silt, and sandy mud, the SR initially increases and then decreases with increasing distance from the continental margin. For smaller particles such as silty mud, mud, sandy clay, silty clay, and clay, the variation in SR with distance may show a complex trend of initially increasing, then decreasing, followed by further increases and decreases (Fig. 7). In proximity to the continental margin, a wide variety of sediments are found, and overall SRs are relatively high (Fig. 7a and b). Within the 120–220 km range from the continental margin, the variety of sediments decreases (Fig. 7c and d), followed by an increase in sediment types in deeper marine areas (Fig. 7e, f, 7g). Subsequently, both the variety of sediments and SRs decline (Fig. 7h and j).

This is partly because, as the distance from the continental margin increases, the pelagic transport of sediments is influenced by various factors, such as interactions with deep-sea gravity flows and sediment re-transportation (Shanmugam, 2000). Larger particles require stronger currents for transport, and these particles typically originate from orogenic zones (Gurnis, 1992). Generally, the farther from the continental margin, the deeper the water and the stronger the hydrodynamic

forces, which differently affect the SRs of these terrigenous clastic sediments (Pan et al., 2016). On the other hand, sand is a non-cohesive material, whereas silt, mud, and clay are cohesive, and their transport processes and interactions with other materials, as well as the extent to which they are influenced by hydrodynamic forces, are complex (McCave, 1984; Cuthbertson et al., 2016). Additionally, the influence of water depth on the SRs of different terrigenous clastic sediments (Fig. S1) is also complex. However, generally speaking, when the distance from the continental margin exceeds 500 km and water depths stabilize near 4000 m, the median SR of these terrigenous clastic sediments tends to be low, less than 10 cm/kyr. Silt, clayey silt, and clay, with SRs across various distances (Fig. 7a-h), are widely present in the ocean, influenced by ocean currents and the resuspension of fine sediments (Lavelle et al., 1984; Ebukanson and Kinghorn, 1990). This distribution pattern relates to significant continental shelf exposure during sea-level glacial periods (Honjo et al., 1982a,b; Chen et al., 2017). In deep basins, restricted circulation conditions initially led to the rapid accumulation of fine terrigenous clasts, which reduced as circulation became more open (Dutkiewicz et al., 2015).

4.3.2. SRs response to biogenic sediments

The SRs of biogenic sediments globally are deeply interconnected with specific sea surface parameters, with distribution varying significantly worldwide (Dutkiewicz et al., 2015). Marine sediments, rich in both terrestrial and biogenic components and often classified as hemipelagic sediments, typically deposit through slow, continuous processes, contrasting with the rapid, intermittent sedimentation observed in phenomena like turbidity currents and landslides (Damuth, 1977).

The distribution and characteristics of biogenic sediments are determined by the biogeography of organisms in surface currents and the chemical composition of seawater, which alters the composition of sediments in deeper areas (Berger, 1967). In marine sediments, the contribution of biogenic material decreases with depth, and biogenic sediments have relatively short residence times in the deep-sea water column. It is expected that there will be minimal dissolution and remineralization upon reaching the deep-sea floor, except for coccolith particles (Honjo et al., 1982a,b). Given the distinct geographical differences between the Northern and Southern Hemispheres and the impact of ancient environmental variations on organism habitats, it is crucial to examine the SRs for different biogenic sediments separately within each hemisphere (Fig. 8). There is a notable hemispherical difference in SRs, particularly between the Southern and Northern Hemispheres. The Northern Hemisphere, closer to larger landmasses and more land at high latitudes, sees more ice sheet formation, contributing to climate cooling through ice-albedo feedback (Anderson et al., 2013). This hemisphere features prevalent marine biogenic siliceous sediments in upwelling zones, indicative of high surface water productivity and influenced by strong ocean currents (Baldauf and Barron, 1990; Gersonde et al., 1999).

In contrast, the Southern Hemisphere, especially at higher latitudes, shows lower SRs compared to equatorial regions, likely due to increased material input from tropical rivers and the development of extensive sea ice around Antarctica, enhancing productivity in Antarctic waters (Goldberg and Griffin, 1964; Hays, 1965). This distinction is evident in the equatorial Atlantic, where average SRs for Globigerina ooze and red clay are notably lower than for diatom ooze, with significant changes observed during the last ice age (Schott, 1939).

4.3.3. SRs response to carbonate sedimentary rocks

Most carbonate sediments in the ocean originate from the weathering of continental materials, with these carbonates being redistributed by deposition on continental shelves, in shallow seas, and on the deep-sea floor (Sclater et al., 1979). The data analysis results in this paper indicate that as the grain size of carbonate rocks decreases (grainstone, packstone, wackestone, mudstone, marl), the median SRs in their box plots progressively increase (Fig. S3). These carbonate sediments display varying SRs and distinct regional characteristics. Our analysis incorporates data from Expeditions 356 and 359, which focused on exploring the history of aridity and monsoon history off coast of Australia and in the central Indian Ocean's Maldives, respectively. These expeditions have significantly enhanced our understanding of these lithologies (Gallagher et al., 2017; Betzler et al., 2017). However, our calculated results do not entirely conform to this expected pattern. Moreover, considering the work of (Bathurst and Tucker, 1990), the probability of carbonate diagenesis occurring within a span of 2.58 Ma is relatively low. This leads us to hypothesize that the carbonate sedimentary rocks in this context did not form during the Quaternary. It is more likely that carbonate calcium biota initially appeared as ooze, rather than forming into solid rocks like grainstone (Choudhari et al., 2023).

Additionally, the SR calculated in our study do not match the anticipated rate based on particle sizes of calcite in the carbonate sedimentary rocks. Although grainstone contains the largest particles, its median SR is relatively low, a pattern also observed in packstone and wackestone. Given that these data are derived from only three expeditions; they may not provide a comprehensive global perspective. As a result, we propose that grainstone and other carbonated sedimentary rocks may have originated in older geological periods. These rocks could have been transported to the Australian coast during the Quaternary, a hypothesis that necessitates further investigation to confirm.

4.4. Semi-quantitative method of SRs

Based on the quantitative results previously discussed, in combination with supplementary data provided in the article (Supplementary Data 5), our analysis has enabled us to draw semi-quantitative inferences regarding lithology and SRs. Specifically, for Quaternary ocean sediments, we have developed a semi-quantitative method that delineates the relationship between SRs and lithology, considering variables such as proximity to continental margins, water depth, ocean characteristics, and latitude. This creative method yields valuable insights crucial for advancing geological research. In the realm of terrestrial clastic sediments, we observe significant variations in SRs across different particle types, including sand, silt, mud, and clay. These variations are not just nominal but show distinct trends at various boundary points. For instance, the most probable SR for clay is concentrated around 5 cm/kyr, whereas for mud, it's approximately 25 cm/kyr. Silt typically has an SR of around 35 cm/kyr, and for sand, the SR is expected to be about 42 cm/kyr. Furthermore, sandy sediments, which encompass silty sand, clayey sand, fine sand, silt, clayey silt, and sandy clay, are predominantly found in the Indian and Pacific Oceans.

When the water depth is less than 1000 m, most terrigenous clastic SR exceed 10 cm/kyr. When the water depth exceeds 4000 m, most terrigenous clastic SRs are less than 10 cm/kyr. At water depths exceeding 5000 m, the sediment type is primarily clay, with SRs below 1 cm/kyr. Within a distance of range from 220 to 250 km from the continental margin, at water depths ranging from 1000 to 2000 m, terrigenous clastic SRs range from 20 to 40 cm/kyr. At distances of range from 300 to 400 km from the continental margin, with water depths ranging from 2500 to 3500 m, terrigenous clastic SRs range from 10 to 40 cm/kyr. At distances of range from 400 to 500 km from the continental margin, with water depths ranging from 3000 to 4000 m, terrigenous clastic SRs are approximately range from 0 to 30 cm/kyr. At distances of range from 500 to 700 km from the continental margin, with water depths between 3000 and 4000 m, terrigenous clastic SRs range from 0 to 10 cm/kyr.

Notably, the SRs in these oceans exhibit significant differences, with the Pacific Ocean generally presenting higher rates. For example, the SR for silty sand in the Indian Ocean mainly ranges from 2 to 20 cm/kyr (the minimum value of the SR range is rounded up and the maximum value is rounded down), while in the Pacific, it predominantly falls between 25 and 60 cm/kyr. Additionally, the SR for clayey sand in the

Indian Ocean hovers mainly around 5 cm/kyr, occasionally reaching up to 43 cm/kyr. In contrast, the Pacific Ocean displays rates around 50 cm/kyr. The SR for fine sand in the Indian Ocean lies between 10 and 12 cm/kyr, whereas in the Pacific, this range expands significantly, varying from 58 to 61 cm/kyr. Sandy silt in the Indian Ocean varies from 2 to 18 cm/kyr, while in the Pacific, it ranges from 20 to 48 cm/kyr. Muddy sediments, including sandy mud, silty mud, and mud, are mainly distributed across the Atlantic and Pacific Oceans, with the Atlantic typically showing higher SRs. For instance, sandy mud in the Atlantic ranges from 17 to 38 cm/kyr, with some instances reaching between 59 and 85 cm/kyr. In contrast, the Pacific Ocean displays a range from 5 to 25 cm/kyr, with occasional readings reaching 43 cm/kyr. In terms of clay distribution, which is a unique sediment type, it is found across the Atlantic, Pacific, Indian, and Southern Oceans. The SRs in these regions are diverse; for example, in the Atlantic, they range from 1 to 14 cm/kyr, in the Indian Ocean from 1 to 25 cm/kyr, occasionally reaching 43 cm/kyr and even 83 cm/kyr. In the Pacific, the rates vary from a low of 0–18 cm/kyr, extending up to 34–67 cm/kyr, while in the Southern Ocean, they range from 0 to 3 cm/kyr. Moreover, finer particles such as silt, clayey silt, and sandy clay are generally present within a range of approximately 700 km from the continental edge. In contrast, sand and silty sand are more commonly found within a closer range of about 120 km from the continental edge, showcasing a broad spectrum of SRs. Interestingly, though sandy mud, silty mud, and mud have smaller particle sizes, they are predominantly distributed in regions nearer to the continental edge, also exhibiting a wide range of SRs. For sediments located beyond 400 km from the continental edge, the SR typically falls below 45 cm/kyr. Sediments positioned beyond 500 km from the continental edge usually have SRs below 20 cm/kyr, and those beyond 700 km typically feature SRs below 5 cm/kyr.

In the case of biogenic sediments, when combining data from Appendix Table 5 and Supplementary Data 5, we find that at low latitudes, calcareous sediments have SRs range from 0 to 17 cm/kyr. In the mid-latitudes of the Northern Hemisphere, calcareous SRs are higher, approximately 1–50 cm/kyr, and siliceous sediments range from 4 to 55 cm/kyr. Conversely, in the mid-latitudes of the Southern Hemisphere, calcareous SRs drop to 0–10 cm/kyr. In the high latitudes of the Northern Hemisphere, siliceous SRs range from 49 to 50 cm/kyr, whereas in the Southern Hemisphere, these rates are lower, around from 0 to 10 cm/kyr.

In summary, this extensive analysis allows us to make preliminary inferences about the SR ranges of terrestrial clastic and biogenic sediments, taking into account factors such as sediment type, oceanic distribution, distance from the continental edge, water depth, latitude, and other relevant factors. These SR values are instrumental in constraining points that are challenging to determine using paleontological dating. Furthermore, the relationship between SR, lithology, water depth and distance provides a valuable reference for scientists in planning and conducting future scientific investigations.

5. Conclusions

This study offers a creative approach in understanding Quaternary Ocean sediments by quantifying SRs and examining their relationships with distance from continental margins and lithology. This research provides new insights into the study of Quaternary Ocean environments and climate. The key conclusions are.

(1) **Quaternary Sedimentation Rates:** This study employed a polynomial fitting method to calculate SR since the Quaternary at 343 globally distributed sites. Subsequently, the average SRs for the five major oceans were determined and a brief analysis of factors influencing SRs was provided. The findings highlight that the magnitude of SRs results from the complex interaction of variation Earth system components. This method offers a more comprehensive understanding of the evolutionary patterns of ocean SRs across continuous temporal and spatial scales. It serves as a valuable reference for gaining insights into the evolution of SRs in deeper geological time.

(2) **Coupling between SR and Distance and Age:** SRs were quantitatively calculated at different time points (0.5 Ma, 1 Ma, 1.5 Ma, 2 Ma, and 2.5 Ma), examining their relationship with the distance from continental margins. The study reveals a logarithmic decrease in SRs with increasing distance. Notably, the sequence of the five time points varies depending on the magnitude (from large to small) of SRs within different distance ranges from the continental margin. However, near the continental margin (less than 670 km), the sequence of time points is 0.5 Ma, 1 Ma, 1.5 Ma and 2.5 Ma. In the deep-sea regions far from the continental margin (greater than 1850 km), these sequence of time points is 2.5 Ma, 0.5 Ma, 2 Ma, 1 Ma and 1.5 Ma. In the intermediate region (670–1850 km), the sequence of time points is very similar. This reflects the different factors influencing SRs within different distance segments and the similar characteristics of influencing factors within the same distance range.

(3) **Coupling between SR and lithology:** A quantitative analysis of SRs with three major lithological classes—terrigenous clastic sediments, biogenic sediments and carbonate sedimentary rocks. Furthermore, for terrigenous clastic sediments, we can observe specific changes in their lithology type, distance from the continental margin, water depth and SR across four-dimensional scales. Terrigenous clastic sediments ending in sand, silt, mud and clay showed specific SR box plot rules. With increasing distance from continental margins, sediment types and SRs gradually transition, with clay being widely distributed. As water depth increases, there are notable differences in the types and SRs of terrigenous clastic sediments. Biogenic SRs exhibit clear latitudinal variations, with a transition from calcium-based to silica-based sediments in both hemispheres, accompanied by corresponding changes in SRs. In the Northern Hemisphere, from low to high latitudes, biogenic sediments transition from calcareous to siliceous, while SRs gradually increase. Conversely, in the Southern Hemisphere, from low to high latitudes, biogenic sediments also transition from calcareous to siliceous, but SRs gradually decrease. This may be related to the habitat preferences of organism and environmental differences between the northern and southern hemisphere. Based on the analysis of SR statistics for carbonate rocks, we speculate that the carbonate rock data we collected may originate from early diagenesis during the early Quaternary, followed by re-transportation to form. Additionally, since the quality of carbonate rock data is relatively low, further research may be needed to validate these conclusions.

(4) **Semi-quantitative method of SRs**: The semi-quantitative method for SRs offers an initial inference and assessment range applicable to both terrigenous clastic sediments and biogenic sediments. This delineation is particularly valuable in challenging locations where dating is difficult. It serves as a beneficial reference point for future scientific expeditions, providing a framework for preliminary analysis. This study on SRs in the Quaternary Ocean can serve as a valuable reference for investigating the SRs of deep-time ocean sediments.

CRediT authorship contribution statement

Tianyu Huang: Writing – original draft & editing, Coding, Methodology, Formal analysis, Data curation. **Chao Ma:** Conceptualization, Writing – review & editing, Methodology, Funding acquisition. **Siding Jin:** Writing – review & editing, Methodology, Investigation, Formal analysis. **Yida Yang:** Validation, Methodology, Formal analysis. **Xiumian Hu:** Writing – review & editing, Supervision, Funding acquisition. **Mingcai Hou:** Writing – review & editing, Supervision, Funding acquisition.

Declaration of competing interest

The authors declare that they have no known competing financial interests or personal relationships that could have appeared to influence the work reported in this paper.

Data availability

Data will be made available on request.

Acknowledgments

This work was financially supported by the National Natural Science Foundation of China (No. 42050102, 42488201, 42172137, and 42050104), the National Key R&D Program of China (Grant No. 2023YFF0804000), and Sichuan Provincial Youth Science & Technology Innovative Research Group Fund (No.2022JDTD0004). This study is a contribution to the Deep-time Digital Earth (DDE) Big Science Program and IGCP 739. In addition, many thanks to Jingxin Jiang of Nanjing University, Can Cai of China University of Geosciences (Beijing) for their assistance during the research process. Many thanks to Pengcheng Zhang, Qingchen Han, Shengjian Zhou, Longgang Ye, Lele Cheng, Qinyao Zhang, Yuyuan Liu, Xueshuang Li, Xinyi Zhang, Jiajia Zhang, Jinghao Li, Zhisong Cao, Hang He, Li Hou, Chenhao Wang, Jianxin Rong, Cheng Gong, Senhao Ren, Xirui Qiao, Zeping Gao of Chengdu University of Technology for their data extraction assistance. We thank the editor and four anonymous reviewers for their valuable comments, which greatly improved the quality of our manuscript.

Appendix A. Supplementary data

Supplementary data to this article can be found online at https://doi.org/10.1016/j.marpetgeo.2024.106900.

References

Anderson, D.E., Goudie, A., Parker, A., 2013. Global Environments through the Quaternary: Exploring Evironmental change[M]. Oxford University Press.
Baas, J.H., Mienert, J., Abrantes, F., et al., 1997. Late Quaternary sedimentation on the Portuguese continental margin: climate-related processes and products. Palaeogeogr. Palaeoclimatol. Palaeoecol. 130 (1–4), 1–23.
Backman, J., Jakobsson, M., Løvlie, R., et al., 2004. Is the central Arctic Ocean a sediment starved basin? Quat. Sci. Rev. 23 (11–13), 1435–1454.
Bacon, M.P., 1984. Glacial to interglacial changes in carbonate and clay sedimentation in the Atlantic Ocean estimated from 230Th measurements. Chem. Geol. 46 (2), 97–111.
Baldauf, J.G., Barron, J.A., 1990. Evolution of biosiliceous sedimentation patterns—eocene through Quaternary: paleoceanographic response to polar cooling [M]. In: Geological History of the Polar Oceans: Arctic versus Antarctic. Springer Netherlands, Dordrecht, pp. 575–607.
Bathurst, Robin GC., Tucker, Maurice E. (Eds.), 1990. Carbonate Diagenesis[M]. Blackwell Scientific Publications.
Bell, M., Walker, M.J.C., 2014. Late Quaternary Environmental Change: Physical and Human perspectives[M]. Routledge, pp. 60–70.
Berger, W.H., 1967. Foraminiferal ooze: solution at depths. Science 156 (3773), 383–385.
Betzler, C., Eberli, G.P., Alvarez Zarikian, C.A., et al., 2017. Expedition 359 summary 359. Betzler, C., Eberli, GP, Alvarez Zarikian, CA, and the Expedition.
Biscaye, P.E., 1965. Mineralogy and sedimentation of recent deep-sea clay in the Atlantic Ocean and adjacent seas and oceans. Geol. Soc. Am. Bull. 76 (7), 803–832.
Chen, Q., Kissel, C., Liu, Z., 2017. Late Quaternary climatic forcing on the terrigenous supply in the northern South China Sea: input from magnetic studies. Earth Planet Sci. Lett. 471, 160–171.
Choudhari, P., Nair, A., Mohan, R., et al., 2023. Variations in the Southern Ocean carbonate production, preservation, and hydrography for the past 41, 500 years: evidence from coccolith and CaCO3 records. Palaeogeogr. Palaeoclimatol. Palaeoecol. 614, 111425.
Clift, P.D., Giosan, L., Blusztajn, J., et al., 2008. Holocene erosion of the Lesser Himalaya triggered by intensified summer monsoon. Geology 36 (1), 79–82.
Cochran, J.R., 1990. Himalayan Uplift, Sea Level, and the Record of Bengal Fan Sedimentation at the ODP Leg 116 Sites.
Cuthbertson, A.J.S., Ibikunle, O., McCarter, W.J., et al., 2016. Monitoring and characterisation of sand-mud sedimentation processes. Ocean Dynam. 66, 867–891.
Damuth, J.E., 1977. Late Quaternary sedimentation in the western equatorial Atlantic. Geol. Soc. Am. Bull. 88 (5), 695–710.
Davies, T.A., Hay, W.W., Southam, J.R., et al., 1977. Estimates of Cenozoic oceanic sedimentation rates. Science 197 (4298), 53–55.
Davies, T.A., Kidd, R.B., Ramsay, A.T.S., 1995. A time-slice approach to the history of Cenozoic sedimentation in the Indian Ocean. Sediment. Geol. 96 (1–2), 157–179.
Diesing, M., 2020. Deep-sea sediments of the global ocean. Earth Syst. Sci. Data 12 (4), 3367–3381.
Donnelly, T.W., 1982. Worldwide continental denudation and climatic deterioration during the late Tertiary: evidence from deep-sea sediments. Geology 10 (9), 451–454.
Dutkiewicz, A., Müller, R.D., O'Callaghan, S., et al., 2015. Census of seafloor sediments in the world's ocean. Geology 43 (9), 795–798.
Dutkiewicz, A., O'Callaghan, S., Müller, R.D., 2016. Controls on the distribution of deep-sea sediments. G-cubed 17 (8), 3075–3098.
Ebukanson, E.J., Kinghorn, R.R.F., 1990. Jurassic mudrock formations of southern England: lithology, sedimentation rates and organic carbon content. J. Petrol. Geol. 13 (2), 221–228.
Ericson, D.B., Wollin, G., 1968. Pleistocene Climates and Chronology in Deep-Sea Sediments: magnetic reversals give a time scale of 2 million years for a complete Pleistocene with four glaciations. Science 162 (3859), 1227–1234.
Gallagher, S.J., Fulthorpe, C.S., Bogus, K., et al., 2017. Expedition 356 methods. Proceedings of the international ocean discovery rogram.1–9.
Gard, G., 1993. Late Quaternary coccoliths at the North Pole: evidence of ice-free conditions and rapid sedimentation in the central Arctic Ocean. Geology 21 (3), 227–230.
Gersonde, R., Hodell, D.A., Blum, P., 1999. Leg 177 summary: southern ocean paleoceanography[C]. In: Proc. Ocean Drill. Program Initial Rep, p. 177.
Goldberg, E.D., Griffin, J.J., 1964. Sedimentation rates and mineralogy in the south atlantic. J. Geophys. Res. 69 (20), 4293–4309.
Gurnis, M., 1992. Rapid continental subsidence following the initiation and evolution of subduction. Science 255 (5051), 1556–1558.
Hay, W.W., Sloan, J.L., Wold, C.N., 1988. Mass/age distribution and composition of sediments on the ocean floor and the global rate of sediment subduction. J. Geophys. Res. Solid Earth 93 (B12), 14933–14940.
Hays, J.D., 1965. Quaternary sediments of the antarctic ocean. Prog. Oceanogr. 4, 117–131.
Honjo, S., Manganini, S.J., Poppe, L.J., 1982a. Sedimentation of lithogenic particles in the deep ocean. Mar. Geol. 50 (3), 199–220.
Honjo, S., Manganini, S.J., Cole, J.J., 1982b. Sedimentation of biogenic matter in the deep ocean. Deep-Sea Res., Part A 29 (5), 609–625.
Ibach, L.E.J., 1982. Relationship between sedimentation rate and total organic carbon content in ancient marine sediments. AAPG (Am. Assoc. Pet. Geol.) Bull. 66 (2), 170–188.
Jakobsson, M., Andreassen, K., Bjarnadóttir, L.R., et al., 2014. Arctic Ocean glacial history. Quat. Sci. Rev. 92, 40–67.
Kolla, V., Biscaye, P.E., Hanley, A.F., 1979. Distribution of quartz in late Quaternary Atlantic sediments in relation to climate. Quat. Res. 11 (2), 261–277.
Latimer, J.C., Filippelli, G.M., 2001. Terrigenous input and paleoproductivity in the Southern Ocean. Paleoceanography 16 (6), 627–643.
Lavelle, J.W., Mofjeld, H.O., Baker, E.T., 1984. An in situ erosion rate for a fine-grained marine sediment. J. Geophys. Res.: Oceans 89 (C4), 6543–6552.
Levitan, M.A., Syromyatnikov, K.V., Kuz'mina, T.G., 2012. Lithological and geochemical characteristics of recent and Quaternary sedimentation in the Arctic Ocean. Geochem. Int. 50, 559–573.
Li, M., Kump, L.R., Hinnov, L.A., et al., 2018. Tracking variable sedimentation rates and astronomical forcing in Phanerozoic paleoclimate proxy series with evolutionary correlation coefficients and hypothesis testing. Earth Planet Sci. Lett. 501, 165–179.
Li, Z., Zhang, Y.G., Torres, M., Mills, B.J., 2023. Neogene burial of organic carbon in the global ocean. Nature 613 (7942), 90–95.
Liu, W., Wang, R., Chen, J., et al., 2012. Late quaternary terrigenous sedimentation in the western Arctic Ocean as exemplified by a sedimentary record from the alpha ridge. Adv. Earth Sci. 27 (2), 209.
Lü, X., Versteegh, G.J.M., Song, J., et al., 2016. Geochemistry of middle holocene sediments from south yellow sea: implications to provenance and climate change. J. Earth Sci. 27, 751–762.
MA, Pengfei, Liu, Zhifei, Shouting, T.U.O., et al., 2021. Present status, characteristics, and compilation significance for the data of Scientific Ocean Drilling. Adv. Earth Sci. 36 (6), 643–662.
McCave, I.N., 1984. Erosion, transport and deposition of fine-grained marine sediments [J]. Geological Society, London, Special Publications 15 (1), 35–69.
Molnar, P., 2001. Climate change, flooding in arid environments, and erosion rates. Geology 29 (12), 1071–1074.
Molnar, P., 2004. Late Cenozoic increase in accumulation rates of terrestrial sediment: how might climate change have affected erosion rates? Annu. Rev. Earth Planet Sci. 32, 67–89.
Molnar, P., England, P., 1990. Late Cenozoic uplift of mountain ranges and global climate change: chicken or egg? nature 346 (6279), 29–34.
Moran, K., Backman, J., Brinkhuis, H., et al., 2006. The cenozoic palaeoenvironment of the arctic ocean. Nature 441 (7093), 601–605.
Pan, Y., Zhang, H., Li, X., et al., 2016. Effects of sedimentation on soil physical and chemical properties and vegetation characteristics in sand dunes at the Southern Dongting Lake region, China. Sci. Rep. 6 (1), 36300.
Pang, X., Chen, C., Zhu, M., et al., 2009. Baiyun movement: a significant tectonic event on Oligocene/Miocene boundary in the northern South China Sea and its regional implications. J. Earth Sci. 20 (1), 49–56.
Peketi, A., Mazumdar, A., Pillutla, S.P.K., et al., 2021. Climatic and tectonic control on the bengal fan sedimentation since the Pliocene. G-cubed 22 (3), e2020GC009448.

Polyak, L., Jakobsson, M., 2011. Quaternary sedimentation in the Arctic Ocean: recent advances and further challenges. Oceanography 24 (3), 52–64.
Polyak, L., Bischof, J., Ortiz, J.D., et al., 2009. Late Quaternary stratigraphy and sedimentation patterns in the western Arctic Ocean. Global Planet. Change 68 (1–2), 5–17.
Raymo, M.E., Ruddiman, W.F., 1992. Tectonic forcing of late Cenozoic climate. nature 359 (6391), 117–122.
Restreppo, G.A., Wood, W.T., Phrampus, B.J., 2020. Oceanic sediment accumulation rates predicted via machine learning algorithm: towards sediment characterization on a global scale. Geo Mar. Lett. 40 (5), 755–763.
Sadler, P.M., 1981. Sediment accumulation rates and the completeness of stratigraphic sections. J. Geol. 89 (5), 569–584.
Salvi, C., Busetti, M., Marinoni, L., et al., 2006. Late quaternary glacial marine to marine sedimentation in the pennell trough (ross sea, Antarctica). Palaeogeogr. Palaeoclimatol. Palaeoecol. 231 (1–2), 199–214.
Schott, W., 1939. Rate of sedimentation of recent deep-sea sediments: Part 6. Special Features of Sediments[J], pp. 409–415.
Schwab, F.L., 1976. Modern and ancient sedimentary basins: comparative accumulation rates. Geology 4 (12), 723–727.
Sclater, J.G., Boyle, E., Edmond, J.M., 1979. A quantitative analysis of some factors affecting carbonate sedimentation in the ocean. Deep Drilling Results in the Atlantic Ocean: Continental Margins and Paleoenvironment 3, 235–248.
Shanmugam, G., 2000. 50 years of the turbidite paradigm (1950s—1990s): deep-water processes and facies models—a critical perspective. Mar. Petrol. Geol. 17 (2), 285–342.
Singh, A.D., Holbourn, A., Kuhnt, W., 2023. Editorial preface to special issue: recent advances in Indian Ocean paleoceanography and paleoclimate. Palaeogeogr. Palaeoclimatol. Palaeoecol., 111443
Tan, M., Wu, F., Ma, H., et al., 2022. Facies Model, Sedimentary Process and Depositional Record of Submarine Fans, and Their Implications[J]. Acta Sedimentologica Sinica 40 (2), 435–449.
Wang, P.X., 2018. Earth System and Evolution. Science Press, Beijing, pp. 278–280.
Whitman, J.M., Davies, T.A., 1979. Cenozoic oceanic sedimentation rates: how good are the data? Mar. Geol. 30 (3–4), 269–284.
Worsley, T.R., Davies, T.A., 1979a. Cenozoic sedimentation in the Pacific Ocean; steps toward a quantitative evaluation. J. Sediment. Res. 49 (4), 1131–1146.
Worsley, T.R., Davies, T.A., 1979b. Sea-level fluctuations and deep-sea sedimentation rates. Science 203 (4379), 455–456.
Zhang, R, Jin, Z, Zhu, R, et al., 2023. Investigation of deposition rate of terrestrial organic-rich shales in China and its implications for shale oil exploration[J]. Oil & Gas Geology 44 (4), 829–845.
Zhang, M., Liu, Z., Xu, S., et al., 2013. Element response to the ancient lake information and its evolution history of argillaceous source rocks in the Lucaogou Formation in Sangonghe area of southern margin of Junggar Basin. J. Earth Sci. 24 (6), 987–996.
Zhang, P., Molnar, P., William, R., 2001. Increased sedimentation rates and grain sizes 2–4 Myr ago due to the influence of climate change on erosion ratesNature4106831891897.
Zhao, S H, Liu, Z F, Chen, Q, et al., 2017. Spatiotemporal variations of deep-sea sediment components and their fluxes since the last glaciation in the northern South China Sea [J]. Science China Earth Sciences 60, 1368–1381.
Zhou, D., Sun, Z., Liao, J., et al., 2009. Filling history and post-breakup acceleration of sedimentation in Baiyun Sag, deepwater northern South China Sea. J. Earth Sci. 20 (1), 160–171.
Zhu, C., Xie, Z., Li, F., 2012. Introduction to Global Change Science[M], vols. 73–80. Science Press, Beijing, pp. 390–412.